Structural, magnetic, magneto-caloric and Mössbauer spectral study of Tb2Fe17 compound synthesized by arc melting

S. Charfeddine, K. Zehani, Lotfi Bessais, A. Korchef

Structural, magnetic, magneto-caloric and Mössbauer spectral study of Tb_2Fe_{17} compound synthesized by arc melting

S. Charfeddine,[1,2] K. Zehani,[1] L. Bessais,[1] and A. Korchef[3]
[1)] *CMTR, ICMPE, UMR7182, CNRS – Université Paris Est, 2-8 rue Henri Dunant F-94320 Thiais, France*
[2)] *LVMU, Centre National de Recherches en Sciences des Matériaux, Technopole de Borj-Cédria, BP 73 Soliman 8027, Tunisia.*
[3)] *College of Science, King Khalid University, Abha, KSA*

We have synthesized the intermetallic Tb_2Fe_{17} compound in hexagonal crystal structure by arc-melting without annealing. X-ray diffraction pattern has been refined by Rietveld method. The crystal structure is hexagonal with $P6_3/mmc$ space group (Th_2Ni_{17}-type). The Mössbauer spectrum of Tb_2Fe_{17} compound has been analyzed with seven magnetic sextets assigned to the inequivalent crystallographic sites. The temperature dependence of magnetization data revealed that Tb_2Fe_{17} exhibits a second-order ferromagnetic to paramagnetic phase transition in the vicinity of Curie temperature (T_C = 412K). The relative cooling power around the magnetic transition and the Arrott plots are also reported.

Keywords: Rare earth alloys and compounds, Magnetization, Curie temperature, 2/17 hexagonal structure, Mössbauer spectrometry, Magnetocaloric effect (MCE), Relative Cooling Power (RCP).

I. INTRODUCTION

The rare earth - transition metal based ($R-T$) intermetallic compounds have been investigated for their interesting magnetic and magnetocaloric properties for several technological applications: high performance permanent magnets, high density magnetic recording, magnetic refrigeration. These materials have taken a special place in the research of new magnetic devices[1–3].

The intermetallic $R-$Fe compounds have been extensively studied during the last years. Dariel *et al.*[4], Orlova *et al.*[5], Landin and Agren[6] and Okamoto[7] studied the $R-$Fe phase diagram, They showed the existence of RFe_2, RFe_3, R_6Fe_{23} and R_2Fe_{17} (R = Dy, Tb) phases.

The Tb_2Fe_{17} has two forms: Tb_2Fe_{17} (rhombohedral $R\bar{3}m$ space group with Th_2Zn_{17}-type structure) and Tb_2Fe_{17} (hexagonal $P6_3/mmc$ space group Th_2Ni_{17}-type structure). Both structures are derivatives of the $CaCu_5$-type structure[4,5,7,8]. A certain regular substitution of R atoms by a dumbbell of two T atoms in the $CaCu_5$ structure, can lead to the Th_2Ni_{17}-type structure following : $3RT_5$ - R + $2T$ = R_2T_{17}[9]. Yanson *et al*[10] showed that the hexagonal structures dominate at or below the molar ratio Tb/Fe = 2/17 (10.5 and 9.5 at.% Tb), while the rhombohedral structure dominates at higher Tb contents (11.5 at.%). The iron rich Tb_2Fe_{17} system is suitable to study $3d$ and $4f$ magnetism and the interaction between them.

The magnetocaloric effect is an intrinsic property of the magnetic materials, based on the heating or cooling (reversibly) of a material according to the applied magnetic field. This property is present in all magnetic compounds. The isothermal magnetic entropy change was obtained from the experimental isothermal magnetization data by using the Maxwell relation[11].

The magnetocaloric properties of rare earths and their alloys have been of great interest. This is explained by the existence of various magnetic structures and various types of transitions in these materials, their high magnetization and the localized nature of their magnetic moment. The wide variety of structures comes from the oscillatory nature of the RKKY interactions (Ruderman-Kittel-Kasuya-Yoshida) between the $4f$ moments of very localized, which may lead to positive or negative couplings according to the distance between the moments. Heavy rare earth elements Tb, Gd to Lu (except Yb) in the lanthanide series, and Y have a hcp crystal structure. In the magnetically ordered state, they have complex structures sometimes resulting in a very interesting magnetocaloric effect.[12,13]

In the present work, we have successfully synthesized the hexagonal phase of the Tb_2Fe_{17} compounds, with the molar ratio (10.5 at. % Tb). The samples have been prepared by arc melting without annealing. A systematic crystallographic study by X-ray diffraction followed by Rietveld refinement has been done in order to identify the phases present in the sample. The local magnetic information on the Fe sites are obtained by Mössbauer spectrometry. The magnetic measurements allowed us to highlight a magnetocaloric effect in this type of samples.

II. EXPERIMENTAL METHODS AND DATA ANALYSIS

As-cast ingots, with Tb_2Fe_{17} nominal compositions, were prepared from high purity elements Fe 99.99%, Tb 99.98% by standard arc-melting technique. In order to homogenize prepared samples three successive melting were performed while increasing the voltage provided by the generator (60 A, 80 A, 80 A). The ingots obtained after melting were broken under an inert argon atmosphere in a glove box. In order to obtain a pure phase, several samples of the binary Tb_2Fe_{17} compound were synthesized by arc-melting technique with different Tb content. A single-phase with 10,5 % at. Tb is obtained by simple melting without need of heat treatment.

X-ray diffraction with Cu radiation has been carried out, at room temperature, on a Brucker diffractometer with an internal Si standard to insure a unit cell parameter accuracy of $\pm 1 \times 10^{-3}$Å. The intensities were measured from $2\theta = 20°$ to $2\theta = 90°$ with a step size of 0.02° and counting time of 192 s per scanning step. The data treatment was made by Rietveld method as implemented in the FullProf computer code, with the assumption of a peak line profile of Thompson-Cox-Hastings allowing multiple phase refinement of each of the coexisting phases[14,15]. The thermal parameters and the occupancies are not refined.

The "goodness-of-fit" indicator R_B is calculated as follows:

$$R_B = \frac{\sum_K |I_K(o) - I_K(c)|}{\sum_K I_K(o)}$$

$I_K(o)$ is the observed Bragg intensity and $I_K(c)$ is the calculated one.

The magnetic measurement was carried out using a DSM-8 MANICS differential sample Magneto-Susceptometer, working on the same principle as a Faraday balance. The sample(under the vacuum) is fixed at the end of a brass rod and then placed in the presence of an external magnetic field gradient perpendicular to the rod. A magneto-optic device detects the force by measuring the torsion angle of a wire. Then, a servo-controlled device applies a compensation force that brings the sample rod back in to its initial position. The magnetic transition temperature in studied systems were determined with $M(T)$ measurements carried out in an applied field of 0.18 Tesla and a heating rate of 5 K/min.

The Mössbauer spectra with absorbers containing 10 mg/cm^2 of natural iron, were collected at 295 K on a constant-acceleration spectrometer with 25 mCi ^{57}Co/Rh source. The spectrometer calibration gives a line-width of 0.25 mm/s for α-Fe. The spectra were fitted according to the procedure discussed below with estimated errors of ± 0.1 T for hyperfine fields $H_{\rm HF}$ and ± 0.005 mm/s for isomer shifts δ and quadrupole shifts 2ε.

III. RESULTS AND DISCUSSION

A. Structure analysis

The R_2T_{17} system can be analyzed as an intergrowth of the $CaCu_5$ and Zr_4Al_3 structures. The hexagonal R_2T_{17} Th_2Ni_{17} type structure ($P6_3/mmc$ space group) and the rhombohedral Th_2Zn_{17}-type structure (space group $R\bar{3}m$) structure are closely related. Their respective stability depends essentially on geometric consideration, *i.e.* the ratio of the atomic radius of the R atom to that of the T atom.

The Rietveld refinement of the XRD pattern corresponding to the bullk Tb_2Fe_{17} compound shows an hexagonal Th_2Ni_{17}-type structure $P6_3/mmc$ space group

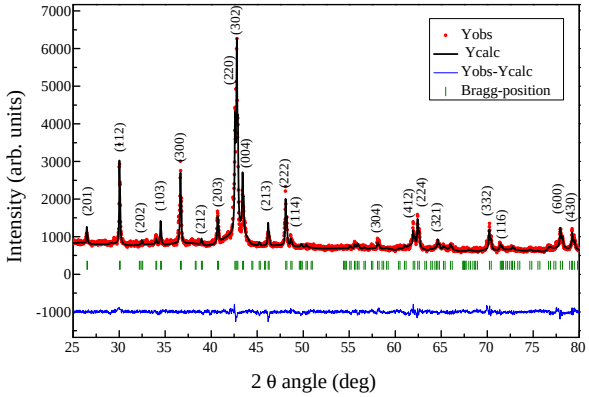

FIG. 1. Observed (dots) and calculated (solid line) XRD pattern of the bulk Tb_2Fe_{17} compound. Vertical bars represent the position of the Bragg reflections. The observed- calculated difference is depicted at the bottom of the figure.

(see figure 1). The Fe atoms occupy four inequivalent crystallographic sites ($12k$, $12j$, $6g$, $4f$ in the Wyckoff site position) and Tb atoms occupy two inequivalent crystallographic sites $2c$ and $2b$ (see figure 2). The hexagonal structure is derived from $CaCu_5$-type structure by the ordered substitution with a pair of Fe-Fe dumbbells ($4g$ site) for each third Tb atom.

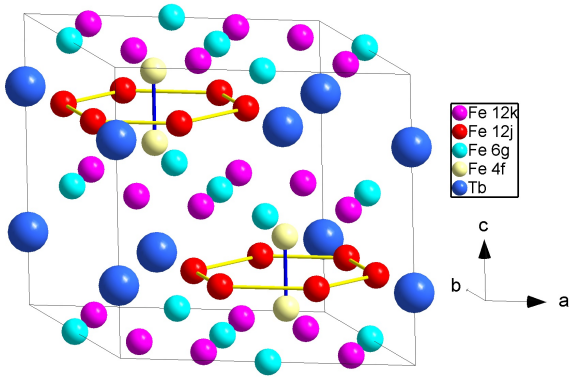

FIG. 2. Crystal structure for the hexagonal $P6_3/mmc$ Tb_2Fe_{17}.

Table I summarizes the crystallographic unit cell parameters, the iron atomic positions as well as the reliability factors of the refinement. These results are in good agreement with those previously reported[16]. Dariel *et al.*[4], Takeda *et al.*[17], and Du *et al.*[18] have synthesized hexagonal Tb_2Fe_{17} compound by different methods, they found a slight difference in unit cell parameters. This difference of the lattice parameters could be due to the effect of annealing step and the melting number and/or to the purity of their phase, especially when taking into account the starting materials purity (99.9%) compared to our samples with 99.99%.

The structural parameters found, for the Tb_2Fe_{17} system will be used for the Wigner-Seitz cell (WSC) volume

TABLE I. a and c cell parameters, R_B and χ^2 factors from Rietveld fit for Tb2Fe$_{17}$.

a (Å)	8.4584(4)
c (Å)	8.3005(4)
c/a	0.9833
V (Å^3)	514.2
χ^2	4.4
R_B	6.87
$x\{12k\}$	0.1667(1)
$x\{12j\}$	0.3520 (3)
$y\{12j\}$	0.3218 (2)
$z\{4f\}$	0.6268 (2)

calculations necessary for a reliable Mössbauer spectrum analysis.

B. Mössbauer spectrometry study

The Mössbauer spectrum of Tb_2Fe_{17}, obtained at room temperature is shown in Fig. 3. It is complex and magnetically ordered spectrum resulting from the convolution of numerous sub-spectra. The existence of four non-equivalent crystallographic sites and the existence of Fe-Fe dumbbells ($4g$ site) connected to the Tb vacancies are responsible for such complexity. In order to analyze that kind of spectrum we need a pertinent physical model connected to the structure characteristics. The site assignment of the hyperfine parameters observed for the crystallographically distinct iron sites in Tb_2Fe_{17} was ruled by : (i) the correlation between the isomer shift (δ) and the Wigner-Seitz cell volume, calculated using crystallographic data derived from Rietveld refinement, (ii) the correlation between the hyperfine field and the near-neighbor environments of the four iron sites.

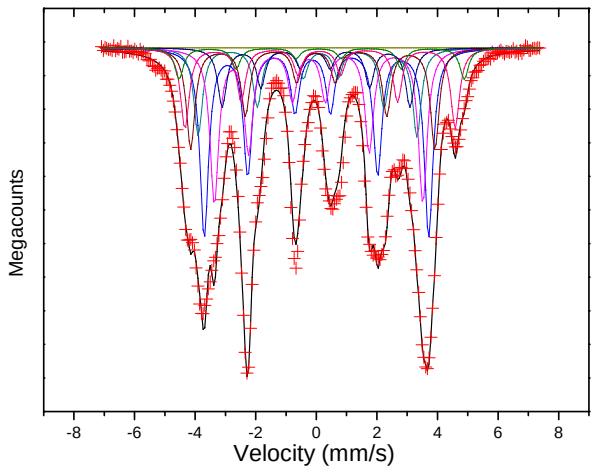

FIG. 3. Room temperature Mössbauer spectrum of Tb_2Fe_{17} compound. The black solid line and the red + symbol scatter plot are the calculated and experimental spectra, respectively. The color solid lines are the seven sextets used in the fit.

TABLE II. Interatomic distances and number of iron near neighbors for the hexagonal $P6_3/mmc$ structure type for Tb_2Fe_{17}. The distances are calculated inside a radius of the coordination sphere equal to 2.81 Å.

Site	Distance (Å)	Number	Notation
12k	2.42(1)	2	12j
	2.44(1)	2	6g
	2.44(1)	2	12k
	2.63(1)	2	12j
	2.66(1)	1	4f
12j	2.42(1)	2	12k
	2.46(1)	1	12j
	2.50(1)	2	6g
	2.63(1)	2	12k
	2.75(1)	1	12j
	2.81(1)	2	4f
6g	2.44(1)	4	12k
	2.50(1)	4	12j
	2.66(1)	2	4f
4f	2.05(1)	1	4f
	2.65(1)	3	12k
	2.66(1)	3	6g
	2.81(1)	6	12j

Hu *et al.*[19] have demonstrated by neutron diffraction that Tb_2Fe_{17} have a basal orientation of the magnetization. Additionally, R. Coehoorn[20] has shown that A_2^0 (the second order crystal field) is negative in the hexagonal Tb_2Fe_{17} compound and α_J (the second-order Stevens factor) is negative for terbium which reinforce the basal orientation of the magnetization. The difference in the hyperfine fields of the crystallographically equivalent but magnetically inequivalent sites results comes mainly from the anisotropy in the orbital field ($3d$ orbital moment) and partly from that in the dipolar field ($3d$ spin moment)[21]. Because of the basal orientation of the Fe magnetic moment in Tb_2Fe_{17}, and the combined effect of the dipolar field and quadrupole interaction, we have used seven magnetic sextets to fit the Mössbauer spectra. Indeed, the four inequivalent iron crystallographic sites $(4f, 6g, 12j, 12k)$ split into seven inequivalent magnetic sites, which are labeled in this case as $4f, 6g_4, 6g_2, 12j_8, 12j_4, 12k_8$, and $12k_4$. As a consequence, seven sextets with the relative areas of 4:4:2:8:4:8:4 are necessary to fit the Mössbauer spectrum (Fig. 3).

It is well demonstrated[15,19,22–29] that for the rhombohedral R_2Fe_{17} compounds, the hyperfine field $H_{\rm HF}$ follows the sequence $6c > 9d > 18f > 18h$, corresponding to the order of the decreasing number of iron near neighbors. Having in mind the geometrical relationship between the iron sites in rhombohedral Th_2Zn_{17} and hexagonal Th_2Ni_{17}: $6c \rightarrow 4f$, $9d \rightarrow 6g$, $18f \rightarrow 12j$, and $18h \rightarrow 12k$, therefore, we expect to obtain the following sequence $4f > 6g > 12j > 12k$ for hyperfine fields. For this purpose, the interatomic distances and the number of iron near neighbors are determined, for the hexagonal $P6_3/mmc$ structure type for Tb_2Fe_{17}, and given in

Table II.

In the first step of the fitting procedure, the hyperfine field assignment to one crystallographic site was based upon the physical fact that the highest fields would belong to $4f$ site according to the number of iron near neighbors. Moreover, the interpretation of the Mössbauer spectrum was based on the relationship between the isomer shift and the Wigner-Seitz cell (WSC) volumes: the larger the WSC volume, the larger the isomer shift[15,25,27,28]. The Wigner-Seitz cell (WSC) volumes have been calculated by means of Dirichlet domains and coordination polyhedra for each crystallographic family using the radius values of 1.80 and 1.26 Å respectively, for Tb and Fe. The WSC volumes resulting from such calculations lead to the following volume sequence: $4f > 12j > 12k > 6g$. In a second step, an average isomer shift value was assigned to each crystallographic family according to the relationship between isomer shift and the WSC sequence. It must be emphasized that the number of the sub-sites used for the fit remains physically significant, as the line-width is equal to 0.27(1) mm/s. In the last step of the fit, all parameters were free.

The results of the calculated Mössbauer spectrum, using our model, showed that the hyperfine fields follow this classification $H_{\rm HF}\{4f\} > H_{\rm HF}\{6g\} > H_{\rm HF}\{12j\} > H_{\rm HF}\{12k\}$ (Table II) in agreement with the number of iron neighbors. The sequence observed for the isomer shift is $\delta\{4f\} > \delta\{12j\} > \delta\{12k\} > \delta\{6g\}$, in agreement with the WSC volume sequence.

Using the conversion factor of 15 T/$\mu_{\rm B}$ for metallic iron we have deduced the average iron magnetic moment $\langle\mu({\rm Fe\ at})\rangle$ equal to 1.63 $\mu_{\rm B}$ (see Table III). Assuming that the Tb magnetic moment $\mu_{\rm Tb} = -4.5\,\mu_{\rm B}$[19], we have calculated the magnetic moment of Tb_2Fe_{17} μ = 18.7 $\mu_{\rm B}$/f.u.

C. Magnetic and magnetocaloric properties

In the intermetallic compounds R_2Fe_{17} the Curie temperature (T_C) is relatively low, around room temperature. It is mainly governed by the interactions between the iron atoms. The nature of these interactions depends on the degree of filling of the Fe 3d band and of the Fe-Fe distances. The reason for the low T_C is that some of the Fe-Fe distances are smaller than the critical value of 2.45 Å needed for ferromagnetic exchange. These Fe pairs couple antiferromagnetically leading to low values of T_C[15,30].

The temperature dependence of the magnetization for the Tb_2Fe_{17} compound in an applied magnetic field of 0.18 T is shown in Fig. 4. One can easily see from this figure the ferromagnetic - paramagnetic transition temperature.

As shown in the inset of the figure, the transition temperature was determined as the minimum of the dM/dT curve. The compound presents a reversible temperature

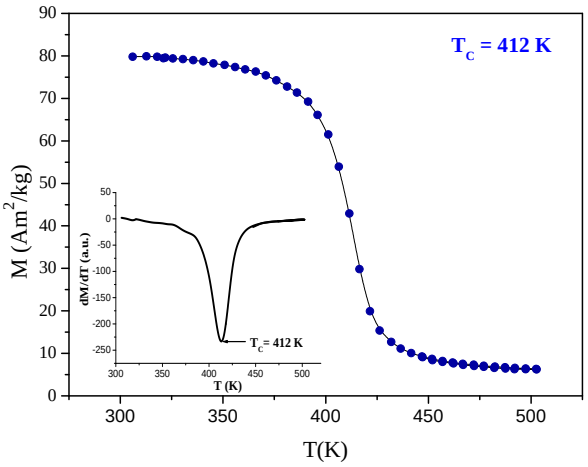

FIG. 4. Temperature dependence of the magnetization for Tb_2Fe_{17} compound. The dM/dT versus T curve (inset).

dependence of the magnetization around the Curie temperature.

The saturation magnetization M_S was estimated by fitting the isothermal magnetization curve $M(H)$. The value of M_S at room temperature is equal to 80.4 Am^2/kg (18.26 μ_B/f.u.) in agreement with the magnetic moment deduced from hyperfine field. These results are consistent with previous results[31]. The magnetization isothermals of Tb_2Fe_{17} between 355 and 440 K are shown in Fig. 5.

Magnetic entropy change ΔS_M was determined as a function of the temperature and the applied magnetic field through the numerical integration of the isothermally measured $M(H)$ curves by means of the following relation[11] :

$$\Delta S_M = \int_0^H \left(\frac{\partial M}{\partial T}\right)_H dH \approx \sum_i \frac{1}{T_{i+1}-T_i}\,(M_{i+1}-M_i)\,\Delta H_i$$

The Arrott plots, deduced from the magnetic field dependence of isothermal magnetization, are shown in figure 6. The positive slope of the Arrott plots for Tb_2Fe_{17} shows that the phase transition from the ferromagnetic state to the paramagnetic state at T_C is a second order phase transition.

Figure 7 illustrates the magnetic entropy change of Tb_2Fe_{17} as a function of temperature and the external field change.

The maximum ΔS_M of Tb_2Fe_{17} is equal to 1.05(3), 1.60(3), 2.19(2) J/kg K, for external field change from 0 to 1.5T. The calculated values for the magnetic entropy change (ΔS_M) in Tb_2Fe_{17} compound in hexagonal crystal structure are higher than those obtained by Chen *et al.* for Tb_2Fe_{17} orthorhombic crystal structure[32].

For magnetocaloric application it is interesting to determine the relative cooling power (RCP). This parame-

TABLE III. Room temperature Mössbauer hyperfine parameters, the WSC volumes and magnetic moment for each iron sites for Tb_2Fe_{17}.

	$4f$	$6g_4$	$6g_2$	$12j_8$	$12j_4$	$12k_8$	$12k_4$	wt. ave.
$\mu_0 H_{\rm HF}$ (T)	29.2(1)	27.7(1)	19.2(1)	25.0(1)	21.3(1)	23.0(1)	22.4(1)	24.4(1)
δ (mm/s)	0.126(5)	-0.093(5)	-0.093(5)	0.112(5)	0.112(5)	-0.056(5)	-0.056(5)	0.006(5)
Q (mm/s)	0.048(5)	0.011(5)	0.013(5)	-0.053(5)	0.161(5)	0.640(5)	-0.216(5)	0.143(5)
WSC volume (Å)	12.49(2)	11.25(2)	11.25(2)	11.73(2)	11.73(2)	11.91(2)	11.91(2)	11.78(2)
μ(Fe at.) (μ_B)	1.94(1)	1.66(1)	1.66(1)	1.58(1)	1.58(1)	1.52(1)	1.52(1)	1.63(1)

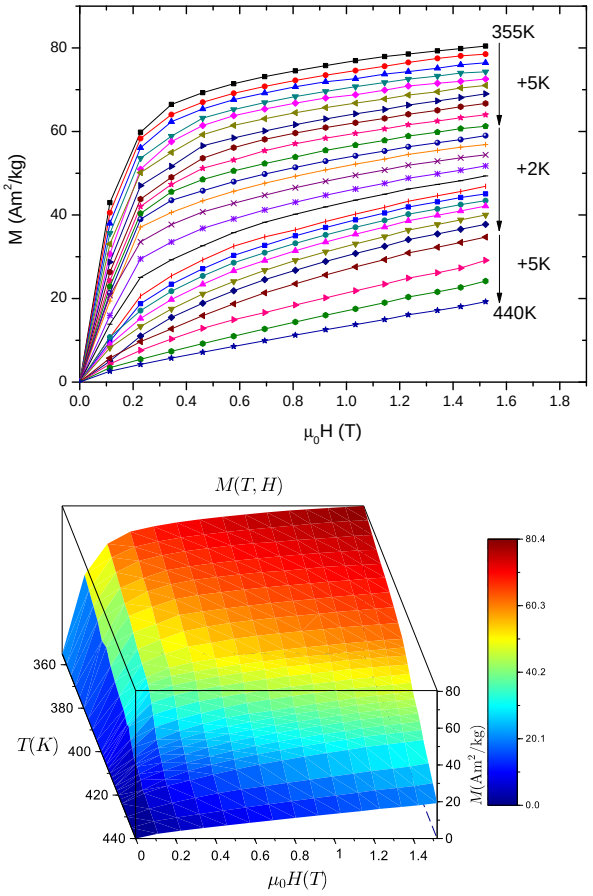

FIG. 5. Isothermal magnetization for Tb_2Fe_{17} compound (left). A 3D surface showing the temperature and applied magnetic field dependencies of the magnetization for Tb_2Fe_{17} compound (right).

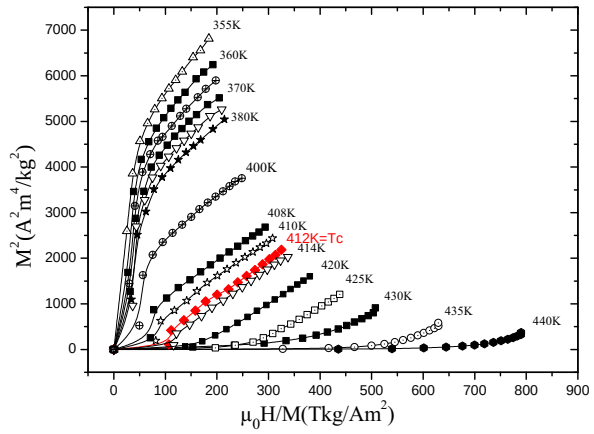

FIG. 6. Arrott plot for Tb_2Fe_{17} over wide range of temperatures 335 K $\leq T \leq$ 440 K.

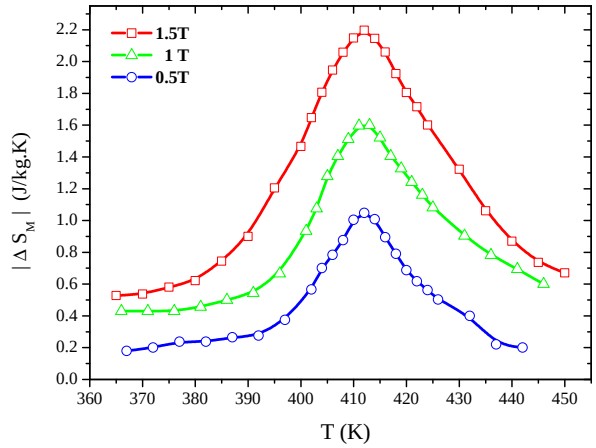

FIG. 7. The magnetic entropy change of Tb_2Fe_{17} as a function of temperature and the external field.

ter is related to the magnetic entropy variation according to the following formula[33] :

$$RCP = -\Delta S_M^{\rm Max} \cdot \delta T^{\rm FWHM}$$

The magnetic entropy change $\Delta S_M^{\rm Max}$ and $\delta T^{\rm FWHM}$ are the maximum of the entropy variation and the full-width at half-maximum in the temperature dependence of the magnetic entropy change ΔS_M. Peaks located at T = 412 K correspond to a direct MCE associated with the magnetic transition from the ferromagnetic to paramagnetic state. The maximum of ΔS_M at $H = 1.5$ T is 2.19 J/kgK, is quite near to the value reported in[34], by Alavarez *et al.* for the system Y_2Fe_{17} and Nd_2Fe_{17}.

Table IV summarizes the magnetocaloric properties: the magnetic entropy change ΔS_M, and the relative cooling power (RCP) calculated for a field up to $H = 1.5$ T. These results have been found as fairly consistent with those found for Pr_2Fe_{17} compounds[1,3,34].

TABLE IV. Magnetic entropy change ΔS_M and relative cooling power RCP for Tb_2Fe_{17}.

Applied field (T)	0.5	1	1.5
ΔS_M (J/kg K)	1.05(3)	1.60(3)	2.19(2)
RCP (J/kg)	28(2)	48(3)	88(3)

IV. CONCLUSION

A single-phase of Tb_2Fe_{17} (with 10,5 % at. of Tb) was obtained by simple arc-melting without any heat treatment.

X-ray powder diffraction shows that the samples crystallize into the ordered hexagonal Th_2Ni_{17}-type structure.

The Mössbauer spectrum of Tb_2Fe_{17}, obtained at room temperature is analyzed using the correlation between the isomer shift (δ) and the Wigner-Seitz cell volume, calculated using crystallographic data derived from Rietveld refinement, and the near-neighbor environments of the four iron sites.

The magnetic properties and the magnetocaloric effect of Tb_2Fe_{17} system have been studied. The magnetic entropy change ΔS_M of the sample was determined. The calculated values for the RCP show that the magnetic entropy changes of Tb_2Fe_{17} are much smaller than that of Gd and some other rare earth intermetallic compounds. Nevertheless, this value of ΔS_M could be interesting for magnetic refrigeration applications and could be interesting for several technological applications using these low-cost iron rich intermetallic compounds.

ACKNOWLEDGEMENTS

This work is mainly supported by the "Ministère de l'Enseignement Suprieur, de la Recherche Scientifique et de la Technologie", University of Carthage, (Tunisia) and the CMTR, ICMPE, UMR7182, Thiais, France.

REFERENCES

[1] R. Guetari, R. Bez, C. B. Cizmas, N. Mliki, and L. Bessais. *J. Alloys Compd.*, 579:156–159, 2013.
[2] R. Grossinger and R. Sato. *J. Magn. Magn. Mater.*, 294:91, 2005.
[3] R. Guetari, R. Bez, A. Belhadj, K. Zehani, A. Bezergheanu, N. Mliki, L. Bessais, and C. B. Cizmas. *J. Alloys Compd.*, 588:64–69, 2014.
[4] M. P. Dariel, J. T. Holthuis, and M. R. Pickus. *J. Less-Common. Met.*, 45:91–101, 1976.
[5] I. G. Orlova, A. A. Eliseev, G. E. Chuprikov, and F. Rukk. *Russian Journal of Inorganic Chemistry*, 22:1387–1389, 1977.
[6] S. Landin and J. Agren. *J. Alloys Compd.*, 207-208:449–453, 1994.
[7] H. Okamoto. *Journal of Phase Equilibria*, 17:80, 1996.
[8] Y. V. Sherbacova, G. E. Ivanova, N. V. Mushinkov, and I. V. Gervasera. *J. Alloys Compd.*, 308:15, 2000.
[9] Y. Khan. *Acta Crystallogr.*, B 30:1533, 1974.
[10] T. Yanson, M. Manyakov, O. Bodak, R. Cerny, and K. Yvon. *J. Alloys Compd.*, 320:108–113, 2001.
[11] M. Foldeaki, R. Chahine, and T. K. Bose. *J. Appl. Phys.*, 77:3528, 1995.
[12] M. Balli, D. Fruchart, D. Gignoux, E. K. Hlil, S. Miraglia, and P. Wolfers. *J. Alloys Compd.*, 442:129–131, 2007.
[13] X. Zhang, L. Yang, S. Zhou, L. Qi, and Z. Liu. *Mater. Trans.*, 42:2622, 2001.
[14] L. Bessais, S. Sab, C. Djega-Mariadassou, N. H. Dan, and N. X. Phuc. *Phys. Rev. B*, 70:134401, 2004.
[15] L. Bessais, E. Dorolti, and C. Djega-Mariadassou. *J. Appl. Phys.*, 97:013902, 2005.
[16] H. Oesterreicher. *J. Less-Common. Met.*, 40:207–219, 1975.
[17] K. Takeda, T. Maeda, and T. Katayama. *J. Alloys Compd.*, 281:50–55, 1998.
[18] J. Du, G. H. Wu, C. C. Tang, Y. X. Li, and W. S. Zhan. *J. Appl. Phys.*, 84:3305, 1998.
[19] Z. Hu, W. B. Yelon, S. Mishra, Gary J. Long, O. A. Pringle, D. P. Middleton, K. H. J. Buschow, and F. Grandjean. *J. Appl. Phys.*, 76:443, 1994.
[20] R. Coehoorn. *Supermagnets, Hard Magnetic Materials*. Kluwer, Dordrecht, 1991.
[21] M. Kawakami, T. Hihara, Y. Koi, and T. Wakiyama. *J. Phys. Soc. Japan*, 33:1591, 1972.
[22] Gary J. Long, O. A. Pringle, F. Grandjean, and K. H. J. Buschow. *J. Appl. Phys.*, 72:4845, 1992.
[23] Gary J. Long, S. Mishra, O.A. Pringle F, Grandjean, and K. H. J. Buschow. *J. Appl. Phys.*, 75:5994, 1994.
[24] C. Djega-Mariadassou and L. Bessais. *J. Magn. Magn. Mater.*, 210:81, 2000.
[25] C. Djega-Mariadassou, L. Bessais, A. Nandra, J. M. Greneche, and E. Burzo. *Phys. Rev. B*, 65:14419, 2001.
[26] I. Nehdi, L. Bessais, C. Djega-Mariadassou, M. Abdellaoui, and H. Zarrouk. *J. Alloys Compd.*, 351:24, 2003.
[27] C. Djega-Mariadassou, L. Bessais, A. Nandra, and E. Burzo. *Phys. Rev. B*, 68:24406, 2003.
[28] L. Bessais, C. Djega-Mariadassou, A. Nandra, M. D. Appay, and E. Burzo. *Phys. Rev. B*, 69:64402, 2004.
[29] L. Bessais, C. Djega-Mariadassou, H. Lassri, and N. Mliki. *J. Appl. Phys.*, 106:103904, 2009.
[30] B. G. Shen, F. W. Wang, L. S. Kong, L. Cao, and Q. Hui. *J. Magn. Magn. Mater.*, 127:L267, 1993.
[31] C. L. Yang, F. S. Li, and W. D. Zhong. *Hyperfine Interactions*, 68, 1991.
[32] H. Chen, Y. Zhang, J. Han, H. Du, Ch. Wang, and Y. Yang. *J. Magn. Magn. Mater.*, 320:1382–1384, 2008.
[33] A. Fujita, , S. Fujieda, and K. Fukamichi. *J. Magn. Magn. Mater.*, 321:3553–3558, 2009.
[34] P. Alavarez, P. Gorria, J. Sanchez-Llamazares, M. J. Perez, V. Franco, M. Reiffers, J. Kovac, I. Puente-Orench, and J. Blanco. *Mater. Chem. Phys.*, 131:18–22, 2011.